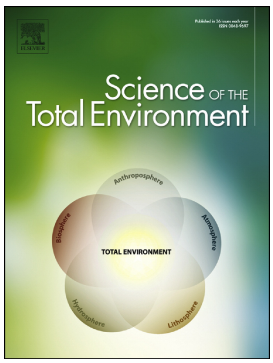

Unsupported Ni metal catalyst in hydrothermal liquefaction of oak wood: Effect of catalyst surface modification

B. de Caprariis, M.P. Bracciale, I. Bavasso, G. Chen, M. Damizia, V. Genova, F. Marra, L. Paglia, G. Pulci, M. Scarsella, L. Tai, P. De Filippis

PII: S0048-9697(19)36211-4

DOI: https://doi.org/10.1016/j.scitotenv.2019.136215

Reference: STOTEN 136215

To appear in: *Science of the Total Environment*

Received date: 11 October 2019

Revised date: 26 November 2019

Accepted date: 18 December 2019

Please cite this article as: B. de Caprariis, M.P. Bracciale, I. Bavasso, et al., Unsupported Ni metal catalyst in hydrothermal liquefaction of oak wood: Effect of catalyst surface modification, *Science of the Total Environment* (2018), https://doi.org/10.1016/j.scitotenv.2019.136215

Unsupported Ni metal catalyst in hydrothermal liquefaction of oak wood: effect of catalyst surface modification

B. de Caprariisa, M.P. Braccialea, I. Bavassoa, G. Chenc, M. Damiziaa, V. Genovab, F. Marrab, L. Pagliab, G. Pulcib, M. Scarsellaa, L. Taia*, P. De Filippisa

a Chemical Engineering Department, Sapienza University of Rome, via Eudossiana 18, 00184, Rome, Italy

b Department of Chemical Engineering, Materials, Environment, Sapienza University of Rome, INSTM Reference Laboratory for Engineering of Surface Treatments, Via Eudossiana 18, Rome 00184, Italy

c School of Environmental Science and Engineering, Tianjin University, Tianjin 300072, China

Abstract

Hydrothermal liquefaction of oak wood was carried out in tubular micro reactors at different temperatures (280-330 °C), reaction times (10-30 min), and catalyst loads (10-50 wt%) using metallic Ni catalysts. For the first time, to enhance the catalytic activity of Ni particles, a coating technique producing a nanostructured surface was used, maintaining anyway the micrometric dimension of the catalyst, necessary for an easier recovery. The optimum conditions for non-catalytic liquefaction tests was determined to be 330 °C and 10 min with the bio-crude yield of 32.88%. The addition of metallic Ni catalysts (Commercial Ni powder and nanostructured surface-modified Ni particle) increased the oil yield and inhibited the char formation through hydrogenation action. Nano modified Ni catalyst resulted in a better catalytic activity in terms of bio-crude yield (36.63%), thanks to the higher surface area due to the presence of flower-like superficial nanostructures. Also, bio-crude quality resulted improved with the use of the two catalysts, with

a decrease of C/H ratio and a corresponding increase of the high heating value (HHV). The magnetic recovery of the catalysts and their reusability was also investigated with good results.

1. Introduction

Along with the economic development and population explosion, the energy demand grows rapidly. Nowadays fossil fuels are still the main energy resource, leading to serious energy shortage and environmental problems. Biomass is considered a promising replacement of fossil fuel due to several advantages such as renewability, neutral CO2 emissions, and worldwide availability. However, widespread energy utilization of biomass is limited by the drawbacks of high moisture content, low energy density, and difficulties in their storage and transportation. Therefore, its transformation into more valuable fuels such as bio-syngas and bio-oil for energy application is considered the most viable way for an efficient biomass exploitation (Ong et al., 2019; Xiong et al., 2017). Within various biomass conversion methods, hydrothermal liquefaction (HTL) is a prospective process (Chan et al., 2019; Kaur et al., 2019).

Usually, HTL of biomass is conducted at medium temperature (250-400°C) and high pressure (40-220 bar) in an oxygen-free reactor with water acting both as reaction medium and reactant (de Caprariis et al., 2019). The process can transform wet biomass into high energy density bio-crude. Comparing with pyrolysis and gasification (operating temperature: 400-900°C), the operating temperature of HTL is lower and no energy-intensive drying process is needed, which leads to less energy input (Tian et al., 2018).

HTL bio-crudes are viscous and dark-colored semi-liquid. The viscosity of the bio-crudes is 10-10, 000 times higher than diesel while the heating values are lower (Ramirez et al., 2015). Therefore, energy expensive upgrading process such as hydrodeoxygenation is always needed. In order to enhance the bio-crude yield and quality, homogeneous and heterogeneous catalysts can be used in the HTL process. Various homogeneous catalysts including alkali hydroxides and metal salts have been extensively tested in the HTL of biomass and a significant increase in the bio-crudes yield with reduced formation of char was observed (Chen et al., 2019; Kumar et al., 2018). However, the separation and reuse of homogeneous

catalyst from aqueous phase is difficult and their use can lead to strong corrosion effect on liquefaction reactor (Yang et al., 2011). Therefore, heterogeneous catalysts including transition metals, zeolites, and transition metal and alkaline earth metal oxides are considered an interesting option to overcome issues related to homogeneous catalysts (Chen et al., 2017; Cheng et al., 2017; Tian et al., 2018; Wang et al., 2018; Wang et al., 2013). Among these catalysts, Ni is frequently used as active specie due to its high activity in a wide range of chemical reactions including hydrogenation, methanation, and steam reforming. Tian et al. reported that the application of Ni/TiO2 catalyst increased the bio-crude yield of HTL of Spirulina from 34.15 wt% to 43.05 wt% (Tian et al., 2018). Younas et al. used NiO nanocatalyst in HTL of rice straw getting the maximum light oil and heavy oil yield up to 13.2 % and 17.2 % at 300 °C (Younas et al., 2017). Chen et al. used Ni modified CeO2 nanorods catalyst in the hydroliquefaction of rice straw and obtained the maximum oil yield of 66.7 % (Chen et al., 2018). Wang et al. used Raney-Ni combined with NaOH in the HTL of biomass at relatively low temperature (245 °C) with water and propanol as solvents. They obtained higher bio-crude yield and also higher HHV of the bio-crude (Wang et al., 2019). The advantage of using metallic Ni with respect to supported catalysts is linked to its magnetic property which makes this catalyst very easy to be recovered. On the contrary, supported catalysts generally are recovered with char by filtration and subsequent combustion of the organic part. This process is high energy consuming and furthermore Ni is recovered as oxide and must be reduced to be used again (Chen et al., 2018; Saber et al., 2016).

The aim of this research is figuring out the effect of Ni metal catalyst on the bio-crude yield and quality obtained by HTL of oak wood. To the best of our knowledge, the use of unsupported metallic Ni as catalyst in the HTL of biomass in absence of hydrogen pressure into the HTL reactor or of a hydrogen transfer agent as co-solvent such as propanol was never reported before.

Furthermore, the modification of the Ni particle surface to enhance its activity was investigated. Ni particle surface was modified by the deposition of a nanostructured pure Ni coating via an electroless nickel plating (ENP) process. ENP consists in the reduction of metal ions in aqueous system without using any external electrical current; the electrons used for the reduction come from the oxidation of a reducing agent in presence of a catalytic surface which is the one to be coated. In comparison with the traditional electrolytic deposition (Feng et al., 2018; Gurrappa & Binder, 2008), electroless plating has some advantages that make it a promising technique for several applications. Electroless plating technique, usually to protect metallic surfaces from corrosion attacks in severe environments and to improve the reinforcement dispersion and compatibility in metallic matrix composites production (Pulci et al., 2014), was never applied in a hydrothermal catalyzed process. This technique allows to overcome the difficulties of making continuous deposition of the coating layer in presence of complex geometry, in this case it is necessary only that the plating solution reaches the overall sample surface. Furthermore, the absence of external applied current allows to have a uniform coating. This peculiar deposition technique, developed by the authors (Genova et al., 2019), involves the growth of a nanostructured coating characterized by a peculiar morphology with the presence of flower like structures. This technique is very promising to enhance the surface area and thus the activity of the catalysts by modification at a nanometric scale of the surface through the presence of sharp nano-spikes without changing its nature. This modification produces also an important effect on wetting properties enhancing the hydrophilic behavior of the particle surfaces (Genova et al., 2019). Furthermore, it allows to work with nanostructures which are known to be more active in catalysis but keeping the overall catalyst particle dimension to a micrometric scale, making the recovery operation easier with respect to catalysts of nanometric particle dimension.

HTL tests were performed on oak wood lignocellulosic biomass using a fixed biomass to water ratio

of 1:5. The influences of temperature (280-330 °C) and reaction time (10-30 min) on bio-crude yield were investigated on HTL tests without catalyst and with commercial Ni powder. Tests with surface modified nanostructured Ni particles, in all the article called Nano-spiked Ni, were conducted only at the operative conditions (temperature and reaction time) which give the highest bio-crude yield. The effect of catalysts load (10-50 % with respect to the biomass weight) was also studied. The catalysts were characterized by scanning electron microscopy (SEM), X-ray diffraction (XRD), and Brunauer-Emmett-Teller (BET) analysis. The bio-crude quality was evaluated with gas chromatography-mass spectrometry (GC-MS) and elemental analysis. The possibility to recover and reuse the commercial Ni powder and Nano-spiked Ni catalysts was also evaluated.

2. Materials and methods

2.1. Materials

Oak wood biomass, collected from farms in the Lazio region in Italy, was grinded and filtered to particle size ranging between 150 and 300 μm. The properties of the oak wood are given in our previous article (de Caprariis et al., 2019). Ni particles were purchased by SIGMA-ALDRICH (powder, <50 μm, 99.7 % trace metals basis) and used without any further purification. All the chemicals, used in the plating process, were purchased from Alfa Aesar (Thermo Fisher Scientific Inc.).

2.2. Catalyst preparation and characterization

2.2.1. Synthesis of Nano-spiked Ni catalyst

The plating bath was obtained by stirring for 30 min at 300 rpm a solution containing hydrazine

(N2H2, 0.8 mol/l) and potassium hydrogen carbonate (KHCO3, 0.45 mol/l) and then adding nickel chloride (NiCl2.6H2O, 0.2 mol/l) in order to form the Ni complex tris(hydrazine carboxylato-N',O) nickelate(1-). A buffer solution of K2HPO4 (0.5 mol/l) was added and the pH was adjusted to a value of 10.9 with KOH. The plating solution was heated at 85 °C by a hotplate IKA RET control-visc (sensitivity ±0.5 °C, temperature sensor PT1000) and pH was controlled with a pH meter METTLER TOLEDO S400 (Genova et al., 2019). Then a specific quantity of Ni particles was added to the as prepared plating solution warmed up to 85 °C and maintained under stirring. After a plating time of 10 min, deionized water was added to stop the reaction. Then, the Nano-spiked Ni particles were filtered, washed with deionized water, and dried overnight at 80 °C. Plating parameters such as temperature T, pH, plating time, stirring rate, and plating ratio defined as to the quantity of solution per grams of Ni particles (Genova et al., 2017) are collected in Table S1.

2.2.2. Catalyst characterization

Morphological analysis of Ni particles (as received and after the electroless plating) was conducted by using a field emission gun-scanning electron microscopy (FEG-SEM) Tescan MIRA3 (EDAX) equipped with a Bruker EDS detector. In order to avoid the adsorption of hydrocarbons naturally present in laboratory air, Nano-spiked Ni catalyst was washed and stored in ethanol and dried before the use as reported elsewhere (Genova et al., 2019).

The crystalline phase of Ni catalysts was assessed by using an X-ray diffractometer (Philips Analytical PW1830) equipped with a Ni-filtered Cu Kα (1.54056 Å) radiation over 30-90° of diffraction angle (2θ) at a scanning speed of 0.008°/min. The data were collected with an acceleration voltage and applied current of 40 kV and 30 mA, respectively. The crystalline phases in the resulting diffractograms

were identified through the COD database (Crystallography Open Database – an open-access collection of crystal structures) (Grazulis et al., 2009). BET analyses were determined following ASTM B922-10 test method (ASTM, 2010). The N2 adsorption isotherms over a p/p0 range from 0.01 to 0.30 were acquired at −196 °C using a Micromeritics 3Flex analyzer (Micromeritics Instrument Corp.). Isotherm analyses were performed using the 3Flex Version 4.05 software. Samples were previously outgassed at 300 °C for 3 h. The BET equation was used to determine the specific surface area.

2.3. Experimental procedure

The experiments were carried out in a 10 mL stainless-steel tubular microreactor. In a typical run, 5 g distilled water and 1 g oak wood were placed in the reactor (biomass to water ratio of 1:5). The catalytic tests were performed with a catalyst biomass ratio ranging between 10 and 50 wt%. The reactor was sealed and purged with nitrogen several times to ensure no air remained inside. The reactor was immersed in sand bath preheated to the setting temperature and shaken by shaft connected to a mechanical stirrer. The range of setting temperatures in this work was 280-330 °C. After the reactor reached the setting reaction temperature (heating rate of about 60 °C/min) it was hold at that temperature for the required time (10-30 min). Finally, the reactor was quenched rapidly with cold water to ambient temperature. For each condition, the experiments were conducted in triplicate.

After cooling the reactor, four products including gas, aqueous phase containing soluble organics, water insoluble organic phase (bio-crude), and solid residue (char and catalyst) were separated using the method described in our previous article (de Caprariis et al., 2017). The gaseous phase was vented off and analyzed with a mass spectrometer (Hayden QGA).

The catalysts in the solid residue were recovered from char magnetically. The detailed procedure is as

follows: an amount of 15 g distilled water and solid residue were mixed in a glass bottle. To separate the char from the catalyst the solution was taken in an ultrasound bath for 30 min. Then a magnet was used to separate the catalyst at the bottom from the suspension of water and char which was removed. This procedure was repeated till the supernatant was clear. Finally, the recovered catalyst was dried at 80 °C for 1 h in the oven. The recovered catalyst showed a purity up to 97 %.

The yields of gas, bio-crude, and char were calculated as follows:

$$Gas\ yield\ (wt\%) = \frac{W_{gas}}{W_{oak\ wood}} \times 100\ \% \quad (1)$$

$$Bio-crude\ yield\ (wt\%) = \frac{W_{bio-crude}}{W_{oak\ wood}} \times 100\ \% \quad (2)$$

$$Char\ yield\ (wt\%) = \frac{W_{char}}{W_{oak\ wood}} \times 100\ \% \quad (3)$$

Where Woak wood is the weight of initial oak wood before reaction, Wgas, Wbio-crude, and Wchar represent the weight of gas, bio-crude, and char obtained after reaction, respectively.

The calorific value of the bio-crudes was calculated with the Dulong formula, the carbon and energy recovery indexes, CR and ER, respectively were calculated as follow:

$$CR\ (oil)\ (\%) = \frac{moles\ of\ C\ in\ bio-crude}{moles\ of\ C\ in\ biomass} \quad (4)$$

$$CR\ (total)\ (\%) = \frac{moles\ of\ C\ in\ bio-crude + moles\ of\ C\ in\ soluble\ organics}{moles\ of\ C\ in\ biomass} \quad (5)$$

$$ER\ (\%) = \frac{\%bio-crude * HHV_{bc}}{HHV_{biomass}} \quad (6)$$

2.4. Product characterization

The chemical composition of bio-crudes was analyzed by GC-MS. GC analysis was performed using a 6890 Model Gas Chromatograph with helium as the carrier gas and a mass spectroscopy detector (Agilent) using a thin film (30 m × 0.32 mm, 0.5 μm film thickness) HP-MS5 capillary column supplied from HP. Bio-crudes were diluted in acetone with dilution ratio 1:10 and subjected to a fixed temperature

ramping profile: 40 °C (held 4 min) to 280 °C at a rate of 10 °C/ min (held 20 min). The injector temperature was 250 °C and the injector split ratio was set to 30:1. Compounds were identified using the NIST spectrum library.

The elemental composition of bio-crudes and bio-chars was measured using a Eurovector EA3000 elemental analyzer. The total organic carbon (TOC) of the aqueous phases was determined using a Shimadzu TOC-L series analyzer.

3. Results and discussion

3.1. Catalyst characterization

SEM analysis of the catalysts (as-received and after electroless plating) are reported in Figure 1a-1d.

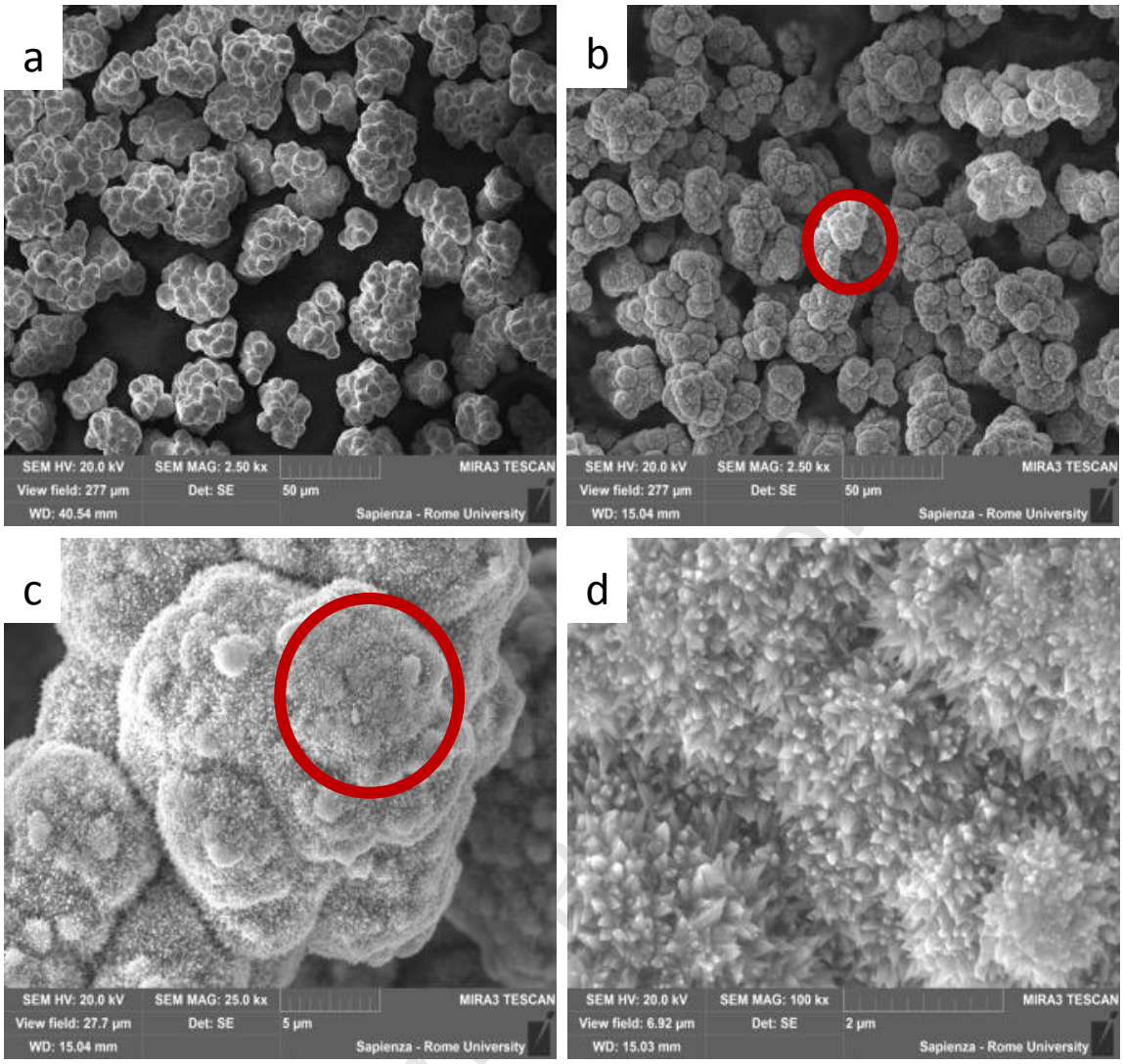

Figure. 1. SEM micrographs of the Ni catalysts. a) as-received; b, c, d) Nano-spiked Ni catalyst at higher magnification (2.5, 25, and 100 Kx, respectively)

The surface modification by electroless nickel plating has not affected drastically the particles dimension and architecture which turns out to be a cluster structure (Fig. 1a, 1b) without any apparent modification. There is no increase in agglomeration of the particles, also after the filtration. The actual surface modification is observed at higher magnification; in Fig. 1 d the flower-shaped structure is shown. This peculiar nanostructure is typical of the electroless pure nickel plating and confirms the success of the nano modification as it was already shown in a previous work for carbon micro fibers (Genova et al., 2017).

The BET results indicate that the used technique for the Ni coating generates an increase in the surface area, from 0.011 m2/g for Ni powder to 0.440 m2/g for the modified one.

3.2. Product distribution

In this section first, the results about the influence of temperature and reaction time on the product yields for tests without catalyst and with Ni powder were reported. The influence of catalyst load was performed at the optimized temperature and reaction time, which gives maximum bio-crude yield, using Ni powder and modified Ni particle.

3.2.1. Effects of reaction temperature

To study the influence of the temperature on the process, tests without and with commercial Ni powder were performed in range of temperature of 280-330 °C. Based on the results obtained in the previous paper the reaction time was set to 15 min and the catalyst biomass ratio to 10 wt% (de Caprariis et al., 2019). The results of the obtained product distribution are reported in Figure 2.

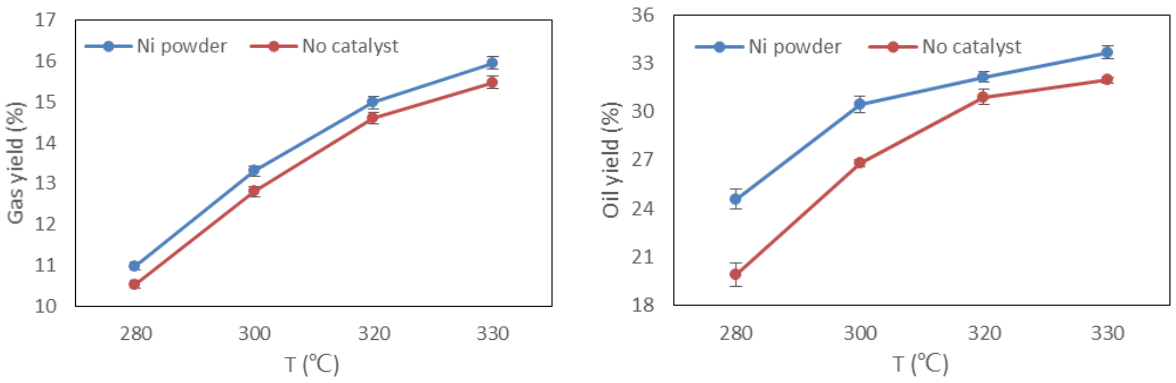

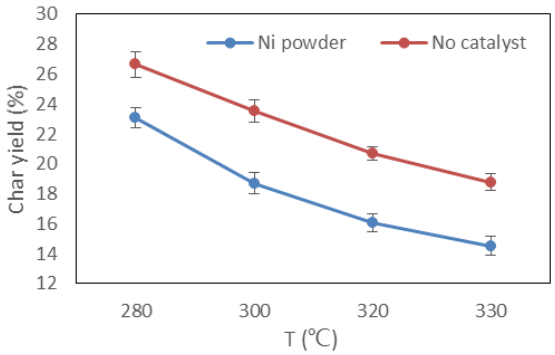

Fig. 2. Effects of reaction temperature on the product distribution (conditions: 15 min, catalyst biomass ratio 10 wt%).

As expected, the increase of temperature leads to an increase of bio-crude and gas yields. The bio-crude raises with the same rate till 320 °C then a little increase is registered between 320 and 330 °C hypothesizing that working over 330 °C is not convenient, as already observed in the previous work (de Caprariis et al., 2019). Thus, the optimum reaction temperature for the catalytic liquefaction of oak wood is considered to be 330 °C. The presence of Ni powder enhances the bio-crude and gas yields: increasing temperature, the bio-crude yields for test without catalyst and with Ni powder range from 19.90 % to 31.95 % and from 24.58 % to 33.68 %, respectively. The effects of Ni catalyst are more evident below 300 °C where bio-crude yield obtained with Ni is about 20 % higher than that obtained without catalyst. When the temperature is increased the depolymerization of the biomass is favored also when no catalyst is used. In this HTL process Ni acts as hydrogenation catalyst utilizing the hydrogen produced from biomass depolymerization. The hydrogenated compounds are more stable and have lower tendency to be recombined and thus repolymerize to give char (Iliopoulou et al., 2012). In fact, a decrease of the char amount from 18.75 % to 14.52 % at 330 °C is observed when Ni is used. The Ni addition also leads to a greater formation of gaseous products, confirming its good catalytic activity both in the hydrocracking and methanation reactions (Duan & Savage, 2011).

As shown in Figure S1 the Ni powder catalyst showed the characteristic reflections of the {111}, {200}, and {220} planes at 44.9°, 52.2°, and 76.7°, respectively, of crystalline Ni. After Ni recovery no diffraction rays corresponding to oxidized Ni element were identified. In order to check the existence of amorphous Ni oxides, energy-dispersive X-ray analysis (EDS) was performed. In the Figure S2, no peak of O element was observed, meaning that in the used conditions the Ni did not undergo oxidation reaction.

3.2.2. Effects of reaction time

The influence of reaction time on oak wood liquefaction product distribution is shown in Figure 3. All these tests were conducted at 330 °C which was identified as the temperature for which the maximum bio-crude yield was achieved. The investigated range of reaction time was 10-30 min keeping constant the catalyst biomass ratio to 10 wt%. Prolonging the reaction time a decrease of the bio-crude yield was observed, while gas and char yields increased in both catalyzed and non-catalyzed tests. Longer reaction times caused a further cracking of the bio-crude products to gas species and a repolymerization to solid residues (Chan et al., 2018; Yan et al., 2019).

With the reaction time extending from 10 min to 30 min, the bio-crude yield obtained using Ni powder decreased from 35.05 % to 29.19 %, while for the non-catalyzed test the yield dropped from 32.88 % to 26.82 %. The highest bio-crude yield of 35.05 % was found at reaction time of 10 min with Ni powder catalyst. Metallic Ni catalyst is supposed to restrain the repolymerization reaction of bio-crude, since due to hydrogenation reactions the low molecular weight compounds, which compose the bio-crude, are more stable and do not tend to be recombined to form char. The gas yield obtained using Ni is higher than in non-catalyzed reaction, in this case the gas production is favored by the presence of Ni which catalyzes the

reforming and methanation, and by the longer reaction time which promotes cracking reactions of bio-crude compounds (Duan & Savage, 2011).

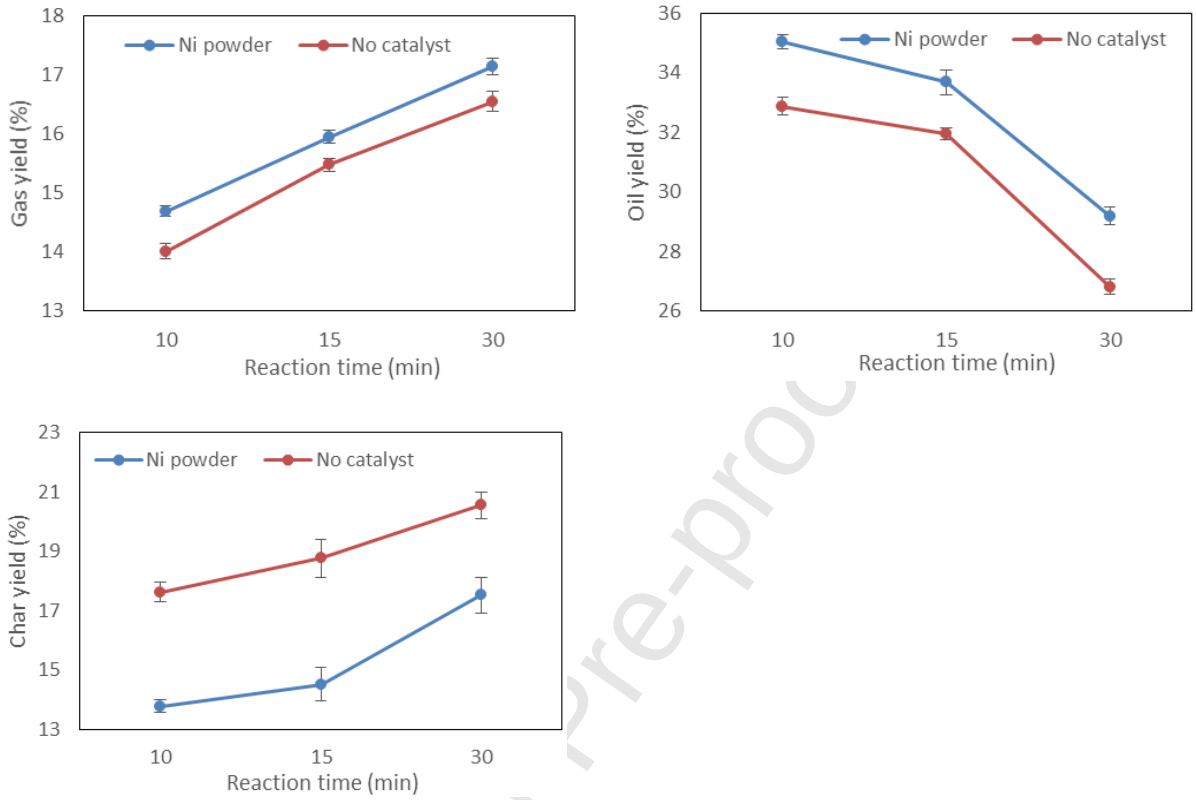

Fig. 3. Effects of reaction time on the product distribution (conditions: 330 °C, catalyst biomass ratio 10 wt%).

3.2.3. Effect of surface catalyst modification

As reported in Table 1, when Nano-spiked Ni catalyst is used the bio-crude yield is 12 % higher with respect to blank test. Also an improvement of 5 % in the oily phase amount is found with respect to Ni powder in the same operative conditions. It is thus evident that the coating of the Ni particles can be considered an effective technique for the enhancement of the Ni activity due to its higher surface area. Furthermore, the enhanced activity of Nano-spiked Ni is confirmed by the higher gas phase amount obtained being the Ni very active, as already said, in the gas formation reactions (Minowa et al., 1998).

Table 1

Product distribution at temperature 330 °C, reaction time 10 min, and catalyst load 10 % wt.

	Bio-crude (%)	Gas (%)	Char (%)
No catalyst	32.88±0.29	14.01±0.13	17.62±0.32
Ni powder	35.05±0.23	14.69±0.09	13.79±0.21
Nano-spiked Ni	36.63±0.19	15.95±0.17	13.02±0.16

3.2.4. Effects of catalyst amount

The amount of catalyst has a great effect on the distribution of the three phases obtained from HTL of oak wood. It is important to find an optimum value for this variable in order to have the optimal catalytic activity for a viable process from an economic point of view. Different amounts of Ni powder catalyst (10 %, 20 %, 30 %, and 50 %) and Nano-spiked Ni catalyst (10 %, 30 %, and 50 %) were used in this research. In Table 2 the yields of gas, bio-crude, and char are shown as a function of different amounts of catalysts for tests performed at 330 °C and 10 min.

For the commercial Ni powder catalyst, the bio-crude yield constantly increased as the catalyst amount raised from 10 % to 50 %. The maximum bio-crude yield was 37.87 % using 50 % Ni powder catalyst, which is 8.05 % and 15.18 % higher than the test with 10 % of catalyst and without catalyst, respectively. The char yield monotonously decreased, and gas yield increased. Although a catalyst to biomass ratio of 50 % leads to the highest bio-crude yield, excessive dosage of catalyst could cause higher operating cost and energy consumption. With Nano-spiked Ni a bio-crude yield of 36.63 % was obtained with 10 % of catalyst while with Ni powder the same value is achieved with an amount three times higher.

These data confirm that the use of the particle nanocoating process, to enhance the catalytic activity of metal particles, can be effective and can lead to savings due to the lower amount of catalyst needed.

Table 2

Product yields of HTL of oak wood with different catalyst loads for tests made at 330 °C and 10 min.

Catalyst (g)	Ni powder				Nano-spiked Ni		
	0.1	0.2	0.3	0.5	0.1	0.3	0.5
Gas yield (%)	14.69±0.09	15.47±0.07	16.05±0.11	17.09±0.13	15.95±0.17	16.79±0.13	17.92±0.15
Oil yield (%)	35.05±0.23	35.75±0.17	36.53±0.11	37.87±0.14	36.63±0.19	37.68±0.22	38.71±0.21
Char yield (%)	13.79±0.21	12.39±0.13	11.77±0.16	9.74±0.20	13.02±0.16	11.22±0.14	8.95±0.29

3.3. Recycling of Nano-spiked Ni catalyst

Recyclability is an important evaluation indicator for catalyst. Reusing catalysts can reduce the operation costs and protect environment. In this research the Nano-spiked Ni catalyst and Ni powder catalyst were recovered from char through ultrasonic water washing and magnet separation, as explained in the previous section, and reused in the HTL of oak wood. The average recovery rates of the Nano-spiked Ni and Ni powder were about 90 %. Bio-crude yields for the experiments using recycled Nano-spiked Ni and Ni powder catalysts are shown in Figure 4. The reusability of Ni powder was proven by these tests since the bio-crude yields remained unchanged. Different results were obtained with Nano-spiked Ni. In fact, the bio-crude yield for the recycled Nano-spiked Ni catalyst was lower of about 2 % than that of the original one after the first reuse, and after the second reuse the catalytic performance was equal to that of

Ni powder catalyst. The reduction of bio-crude yield might be due to the collapse of the Nano picks on the surface of the Nano-spiked Ni catalyst, as demonstrated by the SEM images presented in Figure 5. After first utilization, approximately a quarter of Nano picks were destroyed; this phenomenon was even more emphasized after the second reuse, where the surface of the particles appeared smooth. The particle surfaces were analyzed with EDS in order to exclude the presence of carbon deposits, and actually no significant amounts of carbon were found proving the effectiveness of the recovery process. The collapse of Nano picks, due to mechanical solicitation during the reaction, reduced the surface area of Nano-spiked Ni catalyst decreasing its catalytic efficiency. The recycled Ni powder catalyst was not affected by the use in HTL and presented constant catalytic activity.

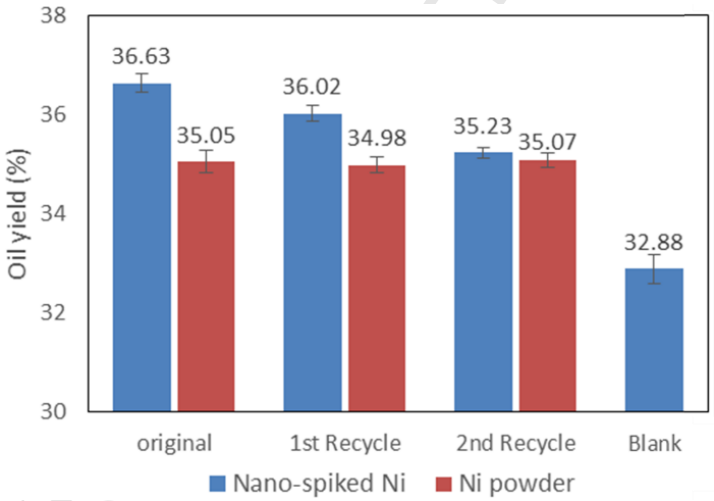

Fig. 4. Bio-crude yields of original and recycled Nano-spiked Ni and Ni powder catalysts.

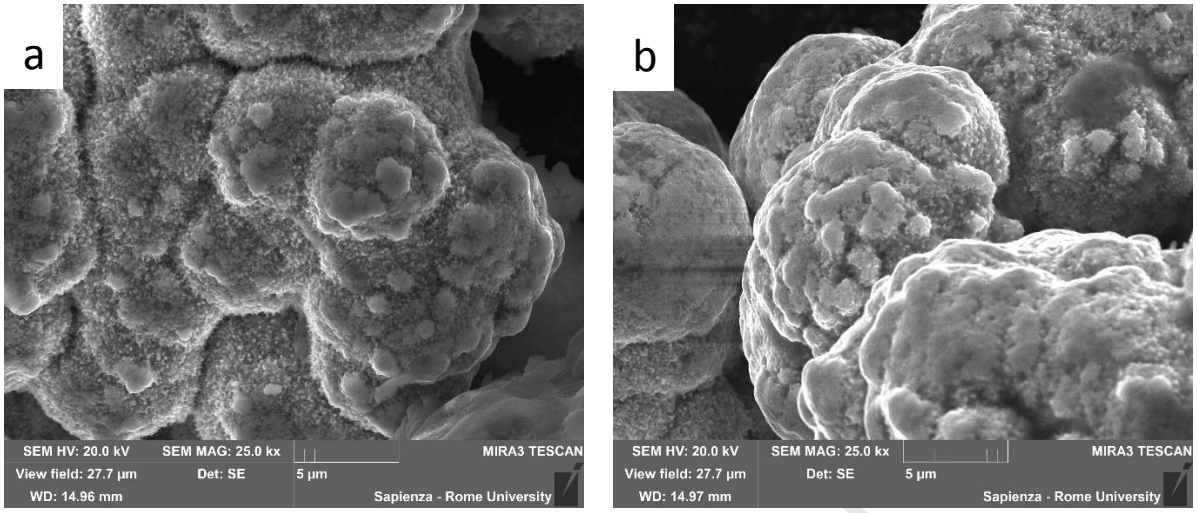

Fig. 5. SEM micrographs of recovered Nano-spiked Ni catalyst (a: after 1st Reuse; b: after 2nd Reuse)

3.4. Product characterization

It is well known that the HTL process, when performed on lignocellulosic biomass in subcritical conditions, leads to different product classes. Owing to the different structure and composition of lignin and holocellulose, the nature and stability of the respective fragments obtained by depolymerization are deeply different. Moreover, the obtained fragments are subjected to different chemical decomposition and modifications (mainly by decarboxylation, dehydration, hydrogenation, and hydrogenolysis) in the reductive conditions given by presence of molecular hydrogen or hydrogen donors. Consequently, a water-soluble light oil is principally obtained from holocellulose, while lignin yields mainly a water insoluble heavy oil (Chen et al., 2017; Kanetake et al., 2007; Moller et al., 2013). Competitive with the above mentioned reactions that lead to more stable products, is the condensation and polymerization process to yield char from the quite instable and highly reactive depolymerization fragments. This process is related, though to a different extent, both holocellulosic and ligninic depolymerization fragments.

The gas analysis is reported in Table 3. As can be noted molecular hydrogen is present in all the gas

fractions, in a relatively relevant percentage. The lower hydrogen percentage and the higher methane content found in the presence of catalysts is attributable to the Ni hydrogenation and methanation activity, respectively (Duan & Savage, 2011).

Table 3

Gas analysis for tests made at 330 °C, reaction time 10 min, and catalyst load 10 wt%.

% vol.	CO2	H2	CH4	VOC
Blank	89.2	1.62	0.61	8.57
Ni powder	91.3	1.14	1.57	5.99
Nano-spiked Ni	92.5	0.85	2.64	4.01

The water phase is characterized by higher amount of soluble organic compounds when catalysts were used (Table 4). Using Nano-spiked Ni catalyst, the water TOC increases of 45 % with respect to the value obtained with blank tests due to the hydrogenation activity of the Ni which stabilizes depolymerized fragments.

Table 4

TOC analysis of the water phase for tests made at 330 °C, reaction time 10 min, and catalyst load 10 wt%.

	TOC (mg/L)
Blank	11571
Ni powder	15328
Nano-spiked Ni	16821

3.4.1. Heavy oil characterization

In Table 5 the results of the elemental analysis are reported. As expected, the bio-crude produced with Ni catalysts has higher amount of hydrogen, leading to a lower C/H ratio which decreased from a C/H of 13.28 in the case of the blank test to 11.51 when an amount of 50 % of Nano-spiked Ni was used. This effect is related to the hydrogenation activity of the Ni in presence of hydrogen. The higher heavy oil yield with the corresponding decrease in the char yield is the result of the Ni-catalyzed hydrogenolytic breaking of lignin bonds (mainly aryl ether bonds) (Song et al., 2013) and of the subsequent stabilization of the primary products obtained from lignin decomposition confirmed by the higher hydrogen amount in the bio-crudes obtained with catalyzed process. This can be principally accounted for the Ni hydrogenation action, mainly on the unsaturated double bonds, while is evident from the high oxygen percentages a minor influence of the catalysts on the hydrodeoxygenation, as well as on the decarboxylation, of the lignin fragments.

The HHV of the bio-crudes is higher with Ni catalysts since more hydrogen is present and rises with the increase of catalyst load. The use of Nano-spiked Ni lets to obtain the highest value of HHV that is about 29 MJ/kg. Furthermore, the presence of the catalysts allows to convert a greater amount of the biomass into bio-crude as demonstrated by carbon recovery values which increases from 46.57 % (blank test) to 54.83 % (50 % of Nano-spiked Ni) and even more, the value reaches 68.29 % (10 % of Nano-spiked Ni) if also the water soluble compounds are considered. The same applies to the energy recovery value which is always positive and increases adding the catalyst. It is interesting to note that with Nano-spiked Ni the values of carbon and energy recovery of 53 % and 50 %, respectively are reached with 30 % of catalysts while 50 % is needed to obtain the same values in the case of Ni powder.

Table 5

Bio-crude characterization: Elemental analysis, HHV, carbon and energy recovery for tests made at 330 °C and reaction time of 10 min.

	C (wt%)	H (wt%)	O (wt%)	C/H	O/C	HHV (MJ/kg)	CR % (oil)	CR % (total)	ER %
Blank	71.1	5.35	23.55	13.28	4.40	27.56	46.57	58.10	42.34
Ni powder 10 %	70.1	5.87	24.03	11.95	4.10	27.87	48.94	64.21	45.64
Ni powder 30 %	70.4	6.03	23.57	11.67	3.91	28.29	51.23		48.30
Ni powder 50 %	70.4	6.05	23.55	11.63	3.89	28.33	53.11		50.13
Nano-spiked Ni 10 %	70.6	6.10	23.30	11.58	3.82	28.50	51.52	68.29	48.79
Nano-spiked Ni 30 %	70.8	6.14	23.06	11.54	3.76	28.67	53.14		50.48
Nano-spiked Ni 50 %	71.1	6.20	22.70	11.51	3.68	28.89	54.83		52.26

The chemical composition of the heavy oil obtained from GC-MS analysis is reported in Table S2. As expected, phenolic compounds account, for every analyzed sample, of more than 68 % of the total area of the compounds detected by GC-MS. In the Figure 6 the percentage area of phenolic compounds bearing an alkyl chain (methyl-, ethyl-, and propyl phenols derivatives plus phenol) and the corresponding ratio with the total phenols % (TP) is reported. The increased presence of these reduced phenolic compounds (PhH) confirms the hydrogenating action of the Ni catalysts on the reactive lignin fragments (Kim et al., 2014). For each tested catalyst concentrations, higher percentages of reduced phenolic compounds are obtained with Nano-spiked Ni, confirming its superior activity. From the ratio PhH/TPh it is possible to evaluate the extent of the catalysts hydrogenating action compared to their action in the breaking of the lignin bonds; namely higher values of PhH/TPh ratio mean that the hydrogenating action is predominant: for low

catalysts amount (10 %) the Nano-spiked Ni appears more active in the hydrogenation of the lignin fragments than the commercial one, while for higher catalyst amounts the activity of the two catalysts is comparable.

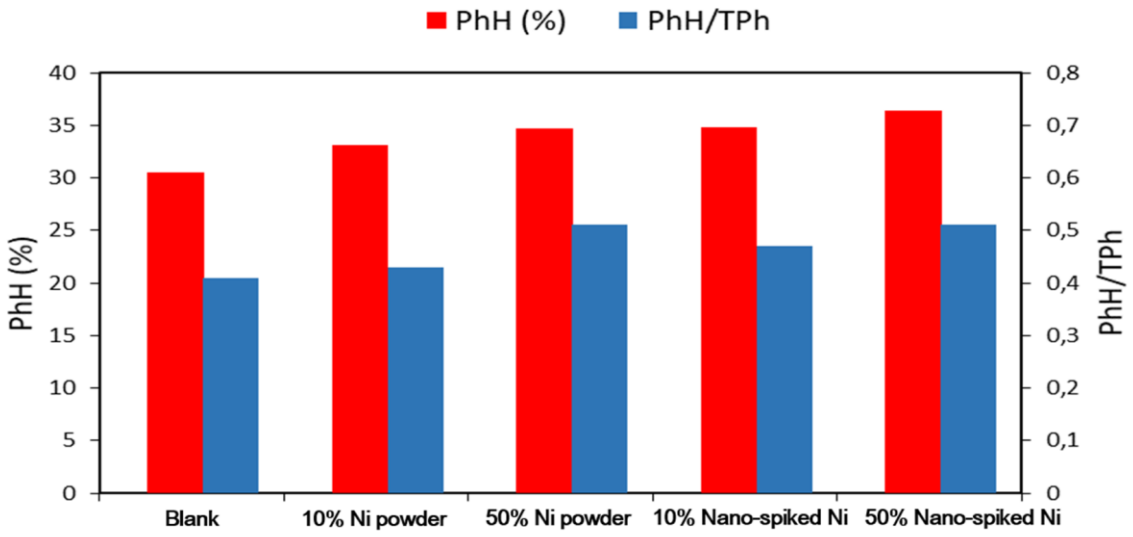

Fig. 6. Percentage area of phenolic compounds with short alkyl chain (PhH) and ratio between PhH and total phenols (TPh) for tests made at 330 °C and reaction time of 10 min with different catalyst loads.

A further evidence of the hydrogenating function of the Ni catalysts is found analyzing the percentages of furfural and furfural derivatives. These compounds, in presence of water and by means of a catalytic hydrogenation step, can be converted into cyclopentanones. In the present reaction conditions, due to the low hydrogen concentration, only cyclopentenones were detected, a reported intermediate in the furfural-cyclopentanone reaction path (Guo et al., 2014; Zhou et al., 2017). In the Figure 7 is evident the higher reduction of furfural and furfural derivatives in the presence of the Ni catalysts and the concurrent higher percentages of the 2-cyclopenten-1-ones. As expected, the catalytic activity on the furfural and furfural derivatives conversion is greater for higher catalysts amounts and for Nano-spiked Ni with respect to commercial Ni powder.

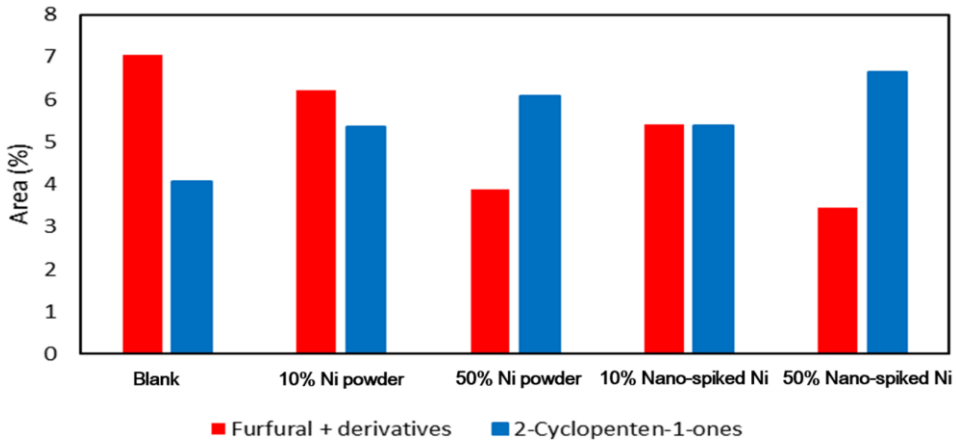

Fig. 7. Percentage area of Furfural and derivatives, and 2-Cyclopenten-1-ones for tests made at 330 °C and reaction time of 10 min with different catalyst loads.

4. Conclusions

The use of unsupported metallic Ni catalysts to improve yield and quality of HTL bio-crude from oak wood was investigated. Ni has the advantage to have magnetic property making its recovery very easy. For the first time, electroless plating process was applied to modify the metal catalyst in order to obtain a nanostructured surface with improved activity. This technique allows to exploit the advantages of nanoscale catalysts maintaining micrometric particles dimension, easier to obtain and to recover. The modified Ni particles have a flower-like superficial structure which results in an increase of the surface area.

The tests were made at 330 °C and 10 min which were found to be the best conditions to obtain the highest oil yields when no catalyst is used (~32 wt%). The addition of Ni catalysts (50 % weight with

respect to biomass) leads to an improvement of bio-crude yield of 16 % when Nano-spiked Ni is used. The Ni, in fact, is a hydrogenation catalyst which acts stabilizing the bio-crude fragments which otherwise can repolymerize to form char. This hydrogenation activity is evident also in the enhancement of the bio-crude quality; the bio-crude obtained with Nano-spiked Ni has an HHV about 10 % higher due to the lower C/H ratio. Furthermore, the hydrogenation function of Ni is demonstrated by the higher presence of 2-cyclopenten-1-ones which comes from the hydrogenation of furfural derivatives.

The modified Ni particles are very promising for the use in catalysis due to their higher activity, in fact lower amount of catalyst (about 40 % less) can be used to obtain same results leading to considerable savings in the overall process.

Easy recovery was demonstrated and also a very good reusability, especially for what concerns Ni powder catalyst; however some further investigations are needed on the modified Ni particles in order to improve their mechanical properties.

References

ADDIN EN.REFLIST ASTM. 2010. Standard Test Method for Metal Powder Specific Surface Area by Physical Adsorption, Vol. ASTM B922-10. America.

Chan, Y.H., Cheah, K.W., How, B.S., Loy, A.C.M., Shahbaz, M., Singh, H.K.G., Yusuf, N.R., Shuhaili, A.F.A., Yusup, S., Ghani, W., Rambli, J., Kansha, Y., Lam, H.L., Hong, B.H., Ngan, S.L. 2019. An overview of biomass thermochemical conversion technologies in Malaysia. *Sci Total Environ*, **680**, 105-123.

Chan, Y.H., Quitain, A.T., Yusup, S., Uemura, Y., Sasaki, M., Kida, T. 2018. Optimization of hydrothermal

liquefaction of palm kernel shell and consideration of supercritical carbon dioxide mediation effect. *Journal Of Supercritical Fluids*, **133**, 640-646.

Chen, D., Ma, Q., Wei, L., Li, N., Shen, Q., Tian, W., Zhou, J., Long, J. 2018. Catalytic hydroliquefaction of rice straw for bio-oil production using Ni/CeO 2 catalysts. *Journal of Analytical and Applied Pyrolysis*, **130**, 169-180.

Chen, S.S., Maneerung, T., Tsang, D.C.W., Ok, Y.S., Wang, C.H. 2017. Valorization of biomass to hydroxymethylfurfural, levulinic acid, and fatty acid methyl ester by heterogeneous catalysts. *Chemical Engineering Journal*, **328**, 246-273.

Chen, Y., Mu, R.T., Yang, M.D., Fang, L.N., Wu, Y.L., Wu, K.J., Liu, Y., Gong, J.L. 2017. Catalytic hydrothermal liquefaction for bio-oil production over CNTs supported metal catalysts. *Chemical Engineering Science*, **161**, 299-307.

Chen, Y.X., Cao, X.D., Zhu, S., Tian, F.S., Xu, Y.Y., Zhu, C.S., Dong, L. 2019. Synergistic hydrothermal liquefaction of wheat stalk with homogeneous and heterogeneous catalyst at low temperature. *Bioresource Technology*, **278**, 92-98.

Cheng, S., Wei, L., Alsowij, M., Corbin, F., Boakye, E., Gu, Z., Raynie, D. 2017. Catalytic hydrothermal liquefaction (HTL) of biomass for bio-crude production using Ni/HZSM-5 catalysts. *AIMS Environmental Science*, **4**(3), 417-430.

de Caprariis, B., Bavasso, I., Bracciale, M.P., Damizia, M., De Filippis, P., Scarsella, M. 2019. Enhanced bio-crude yield and quality by reductive hydrothermal liquefaction of oak wood biomass: Effect of iron addition. *Journal of Analytical and Applied Pyrolysis*, **139**, 123-130.

de Caprariis, B., De Filippis, P., Petrullo, A., Scarsella, M. 2017. Hydrothermal liquefaction of biomass: Influence of temperature and biomass composition on the bio-oil production. *Fuel*, **208**, 618-625.

Duan, P.G., Savage, P.E. 2011. Hydrothermal Liquefaction of a Microalga with Heterogeneous Catalysts. *Industrial & Engineering Chemistry Research*, **50**(1), 52-61.

Feng, J., Gao, C.B., Yin, Y.D. 2018. Stabilization of noble metal nanostructures for catalysis and sensing. *Nanoscale*, **10**(44), 20492-20504.

Genova, V., Marini, D., Valente, M., Marra, F., Pulci, G. 2017. Nanostructured Nickel Film Deposition on Carbon Fibers for Improving Reinforcement-matrix Interface in Metal Matrix Composites. *CHEMICAL ENGINEERING TRANSACTIONS*, **60**, 73-78.

Genova, V., Paglia, L., Marra, F., Bartuli, C., Pulci, G. 2019. Pure thick nickel coating obtained by electroless plating: Surface characterization and wetting properties. *Surface & Coatings Technology*, **357**, 595-603.

Grazulis, S., Chateigner, D., Downs, R.T., Yokochi, A.F.T., Quiros, M., Lutterotti, L., Manakova, E., Butkus, J., Moeck, P., Le Bail, A. 2009. Crystallography Open Database - an open-access collection of crystal structures. *Journal Of Applied Crystallography*, **42**, 726-729.

Guo, J.H., Xu, G.Y., Han, Z., Zhang, Y., Fu, Y., Guo, Q.X. 2014. Selective Conversion of Furfural to Cyclopentanone with CuZnAl Catalysts. *Acs Sustainable Chemistry & Engineering*, **2**(10), 2259-2266.

Gurrappa, I., Binder, L. 2008. Electrodeposition of nanostructured coatings and their characterization-A review. *Sci Technol Adv Mater*, **9**(4), 043001.

Iliopoulou, E.F., Stefanidis, S.D., Kalogiannis, K.G., Delimitis, A., Lappas, A.A., Triantafyllidis, K.S. 2012. Catalytic upgrading of biomass pyrolysis vapors using transition metal-modified ZSM-5 zeolite. *Applied Catalysis B-Environmental*, **127**, 281-290.

Kanetake, W.T., Sasaki, M., Goto, M. 2007. Decomposition of a lignin model compound under hydrothermal conditions. *Chemical Engineering & Technology*, **30**(8), 1113-1122.

Kaur, R., Gera, P., Jha, M.K., Bhaskar, T. 2019. Optimization of process parameters for hydrothermal conversion of castor residue. *Sci Total Environ*, **686**, 641-647.

Kim, K.H., Brown, R.C., Kieffer, M., Bai, X.L. 2014. Hydrogen-Donor-Assisted Solvent Liquefaction of Lignin to Short-Chain Alkylphenols Using a Micro Reactor/Gas Chromatography System. *Energy & Fuels*, **28**(10), 6429-6437.

Kumar, M., Olajire Oyedun, A., Kumar, A. 2018. A review on the current status of various hydrothermal technologies on biomass feedstock. *Renewable and Sustainable Energy Reviews*, **81**, 1742-1770.

Minowa, T., Zhen, F., Ogi, T. 1998. Cellulose decomposition in hot-compressed water with alkali or nickel catalyst. *The Journal of Supercritical Fluids*, **13**, 253-259.

Moller, M., Harnisch, F., Schroder, U. 2013. Hydrothermal liquefaction of cellulose in subcritical water-the role of crystallinity on the cellulose reactivity. *Rsc Advances*, **3**(27), 11035-11044.

Ong, H.C., Chen, W.H., Farooq, A., Gan, Y.Y., Lee, K.T., Ashokkumar, V. 2019. Catalytic thermochemical conversion of biomass for biofuel production: A comprehensive review. *Renewable & Sustainable Energy Reviews*, **113**.

Pulci, G., Tirillo, J., Marra, F., Sarasini, F., Bellucci, A., Valente, T., Bartuli, C. 2014. High Temperature Oxidation and Microstructural Evolution of Modified MCrAlY Coatings. *Metallurgical And Materials Transactions a-Physical Metallurgy And Materials Science*, **45A**(3), 1401-1408.

Ramirez, J.A., Brown, R.J., Rainey, T.J. 2015. A Review of Hydrothermal Liquefaction Bio-Crude Properties and Prospects for Upgrading to Transportation Fuels. *Energies*, **8**(7), 6765-6794.

Saber, M., Golzary, A., Hosseinpour, M., Takahashi, F., Yoshikawa, K. 2016. Catalytic hydrothermal liquefaction of microalgae using nanocatalyst. *Applied Energy*, **183**, 566-576.

Song, Q., Wang, F., Cai, J.Y., Wang, Y.H., Zhang, J.J., Yu, W.Q., Xu, J. 2013. Lignin depolymerization (LDP) in

alcohol over nickel-based catalysts via a fragmentation-hydrogenolysis process. *Energy Environmental Science*, **6**, 994-1007.

Tian, W., Liu, R., Wang, W., Yin, Z., Yi, X. 2018. Effect of operating conditions on hydrothermal liquefaction of Spirulina over Ni/TiO2 catalyst. *Bioresour Technol*, **263**, 569-575.

Wang, W., Xu, Y., Wang, X., Zhang, B., Tian, W., Zhang, J. 2018. Hydrothermal liquefaction of microalgae over transition metal supported TiO2 catalyst. *Bioresour Technol*, **250**, 474-480.

Wang, Y., Wang, H., Lin, H.F., Zheng, Y., Zhao, J.S., Pelletier, A., Li, K.C. 2013. Effects of solvents and catalysts in liquefaction of pinewood sawdust for the production of bio-oils. *Biomass & Bioenergy*, **59**, 158-167.

Wang, Y.L., Pan, X.J., Ye, Y.Y., Li, S.R., Wang, D., Liu, Y.Q. 2019. Process optimization of biomass liquefaction in isopropanol/water with Raney nickel and sodium hydroxide as combined catalysts. *Biomass & Bioenergy*, **122**, 305-312.

Xiong, X.N., Yu, I.K.M., Cao, L.C., Tsang, D.C.W., Zhang, S.C., Ok, Y.S. 2017. A review of biochar-based catalysts for chemical synthesis, biofuel production, and pollution control. *Bioresource Technology*, **246**, 254-270.

Yan, L., Wang, Y., Li, J., Zhang, Y., Ma, L., Fu, F., Chen, B., Liu, H. 2019. Hydrothermal liquefaction of Ulva prolifera macroalgae and the influence of base catalysts on products. *Bioresource Technology*, **292**, 121286.

Yang, C., Jia, L., Chen, C., Liu, G., Fang, W. 2011. Bio-oil from hydro-liquefaction of Dunaliella salina over Ni/REHY catalyst. *Bioresour Technol*, **102**(6), 4580-4.

Younas, R., Hao, S., Zhang, L., Zhang, S. 2017. Hydrothermal liquefaction of rice straw with NiO nanocatalyst for bio-oil production. *Renewable Energy*, **113**, 532-545.

Zhou, M.H., Li, J., Wang, K., Xia, H.H., Xu, J.M., Jiang, J.C. 2017. Selective conversion of furfural to

cyclopentanone over CNT-supported Cu based catalysts: Model reaction for upgrading of bio-oil. *Fuel*, **202**, 1-11.

Declaration of interests

☒ The authors declare that they have no known competing financial interests or personal relationships that could have appeared to influence the work reported in this paper.

☐The authors declare the following financial interests/personal relationships which may be considered as potential competing interests:

Graphical abstract

Highlights

- Unsupported Ni catalyst enhances HTL bio-crude yield and quality.
- Nanostructured Nickel coating improves Ni powder activity
- Electroless plating is effective in modifying surface properties of metal catalyst

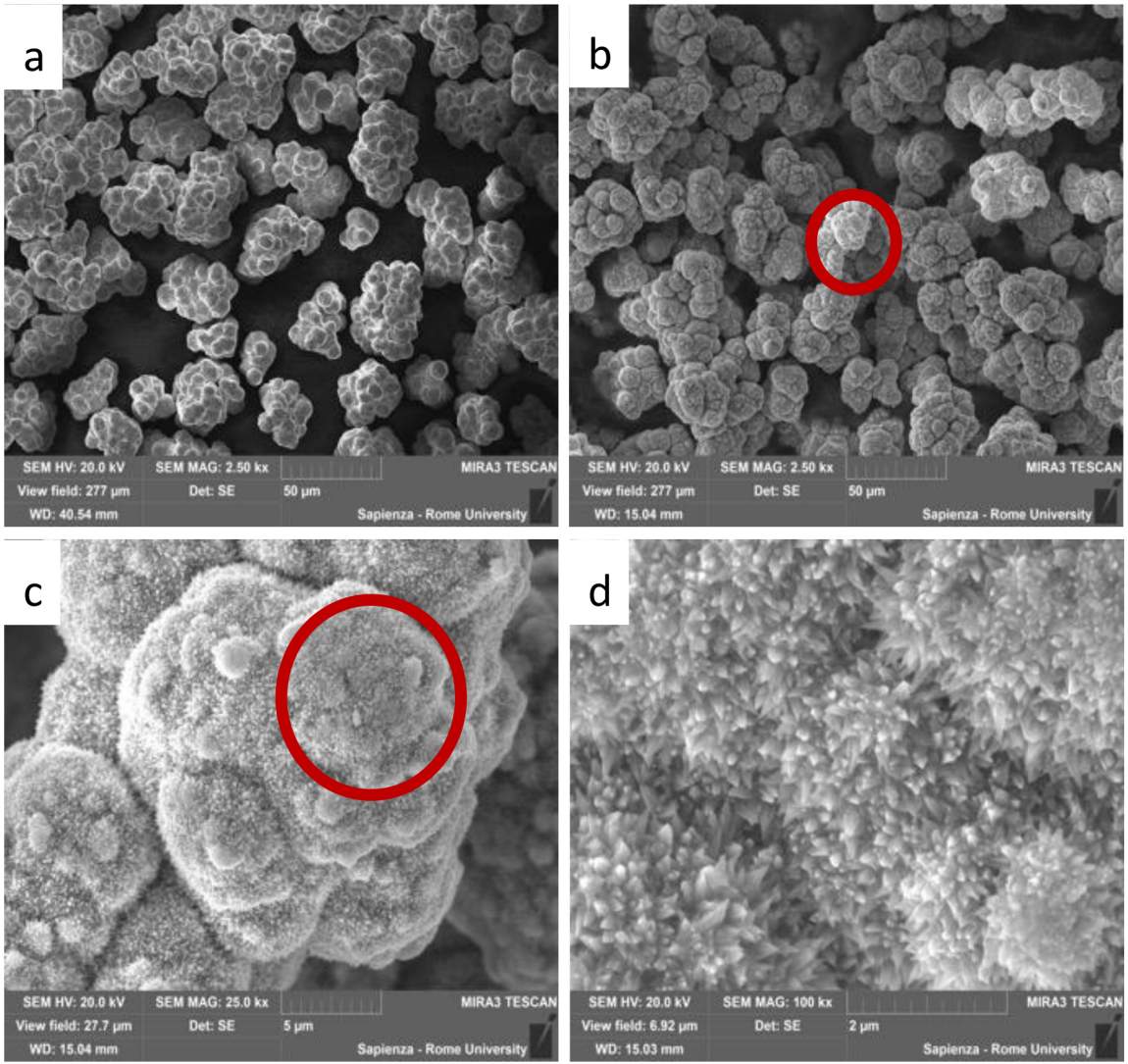
a
SEM HV: 20.0 kV
SEM MAG: 2.50 kx
MIRA3 TESCAN
View field: 277 µm
Det: SE
50 µm
WD: 40.54 mm
Sapienza - Rome University
b
SEM HV: 20.0 kV
SEM MAG: 2.50 kx
MIRA3 TESCAN
View field: 277 µm
Det: SE
50 µm
WD: 15.04 mm
Sapienza - Rome University
c
SEM HV: 20.0 kV
SEM MAG: 25.0 kx
MIRA3 TESCAN
View field: 27.7 µm
Det: SE
5 µm
WD: 15.04 mm
Sapienza - Rome University
d
SEM HV: 20.0 kV
SEM MAG: 100 kx
MIRA3 TESCAN
View field: 6.92 µm
Det: SE
2 µm
WD: 15.03 mm
Sapienza - Rome University

Figure 1

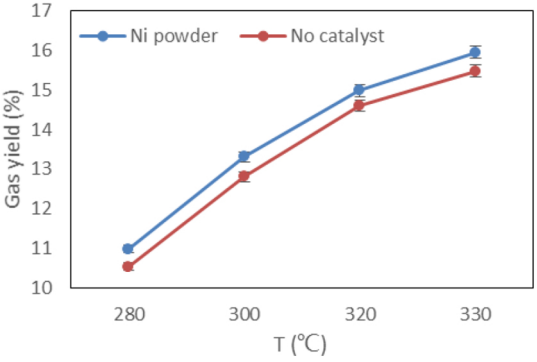
Ni powder
No catalyst
Gas yield (%)
17
16
15
14
13
12
11
10
280
300
320
330
T (℃)

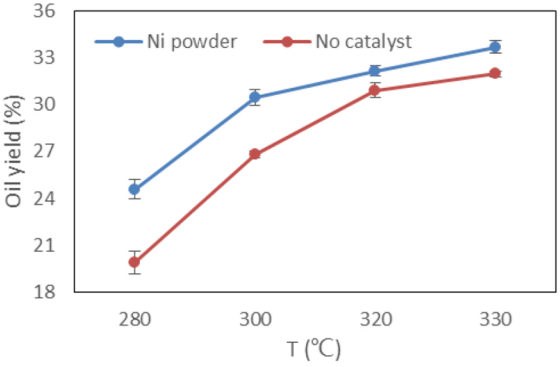
Ni powder
No catalyst
Oil yield (%)
36
33
30
27
24
21
18
280
300
320
330
T (℃)

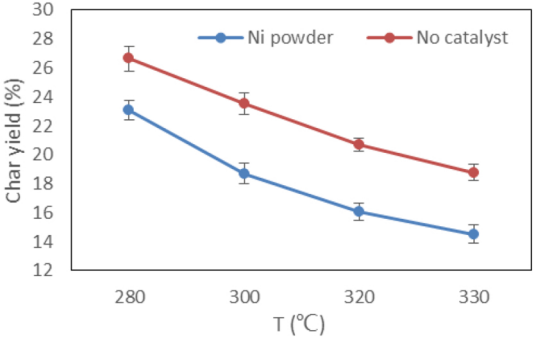
Ni powder
No catalyst
Char yield (%)
30
28
26
24
22
20
18
16
14
12
280
300
320
330
T (℃)

Figure 2

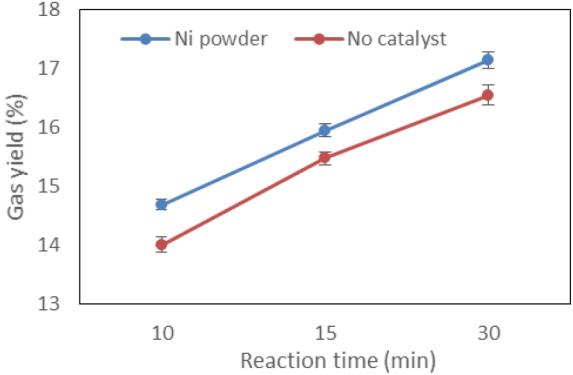
Ni powder
No catalyst
Gas yield (%)
18
17
16
15
14
13
10
15
30
Reaction time (min)

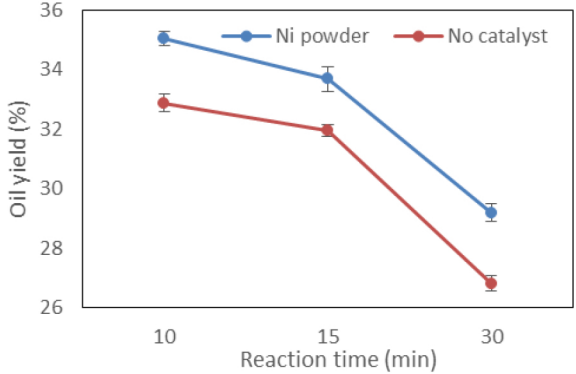
Ni powder
No catalyst
Oil yield (%)
36
34
32
30
28
26
10
15
30
Reaction time (min)

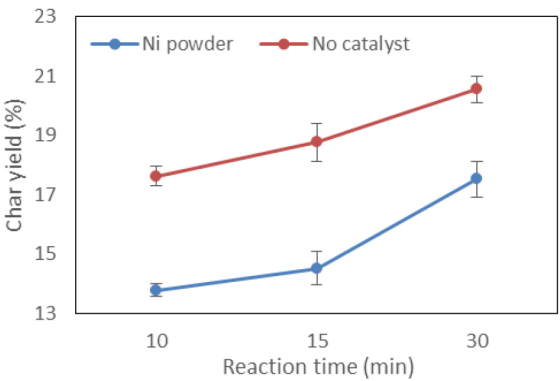
Ni powder
No catalyst
Char yield (%)
23
21
19
17
15
13
10
15
30
Reaction time (min)

Figure 3

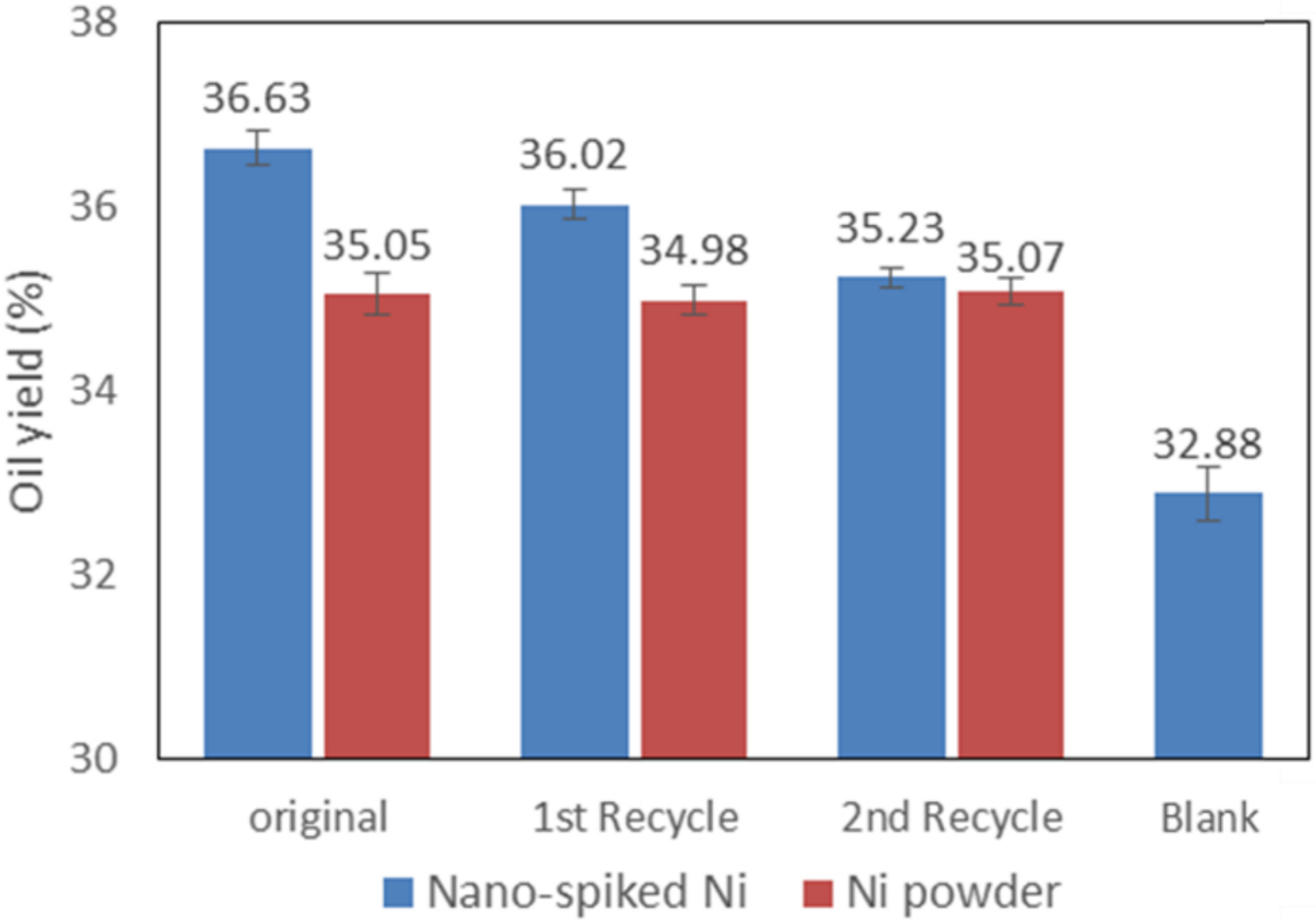
38
36
34
32
30
Oil yield (%)
36.63
35.05
36.02
34.98
35.23
35.07
32.88
original
1st Recycle
2nd Recycle
Blank
Nano-spiked Ni
Ni powder

Figure 4

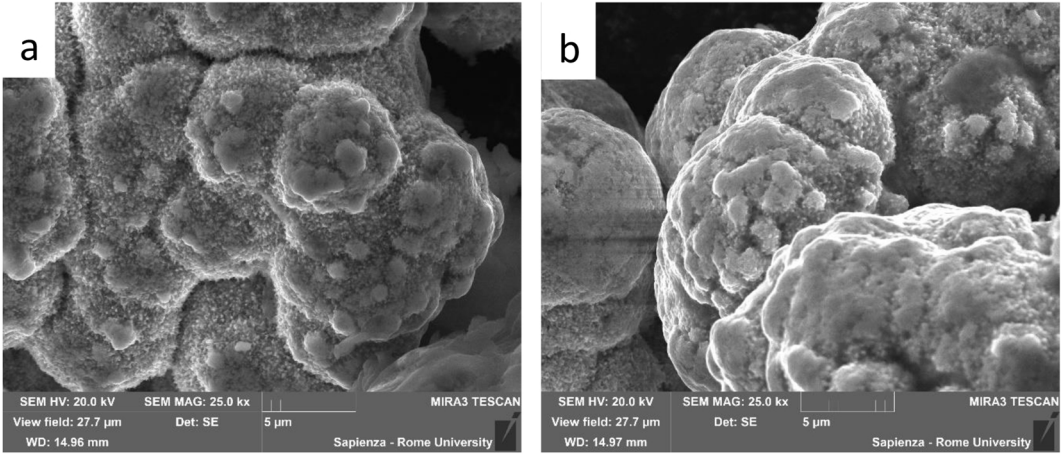
a
SEM HV: 20.0 kV
SEM MAG: 25.0 kx
MIRA3 TESCAN
View field: 27.7 µm
Det: SE
5 µm
WD: 14.96 mm
Sapienza - Rome University
b
SEM HV: 20.0 kV
SEM MAG: 25.0 kx
MIRA3 TESCAN
View field: 27.7 µm
Det: SE
5 µm
WD: 14.97 mm
Sapienza - Rome University

Figure 5

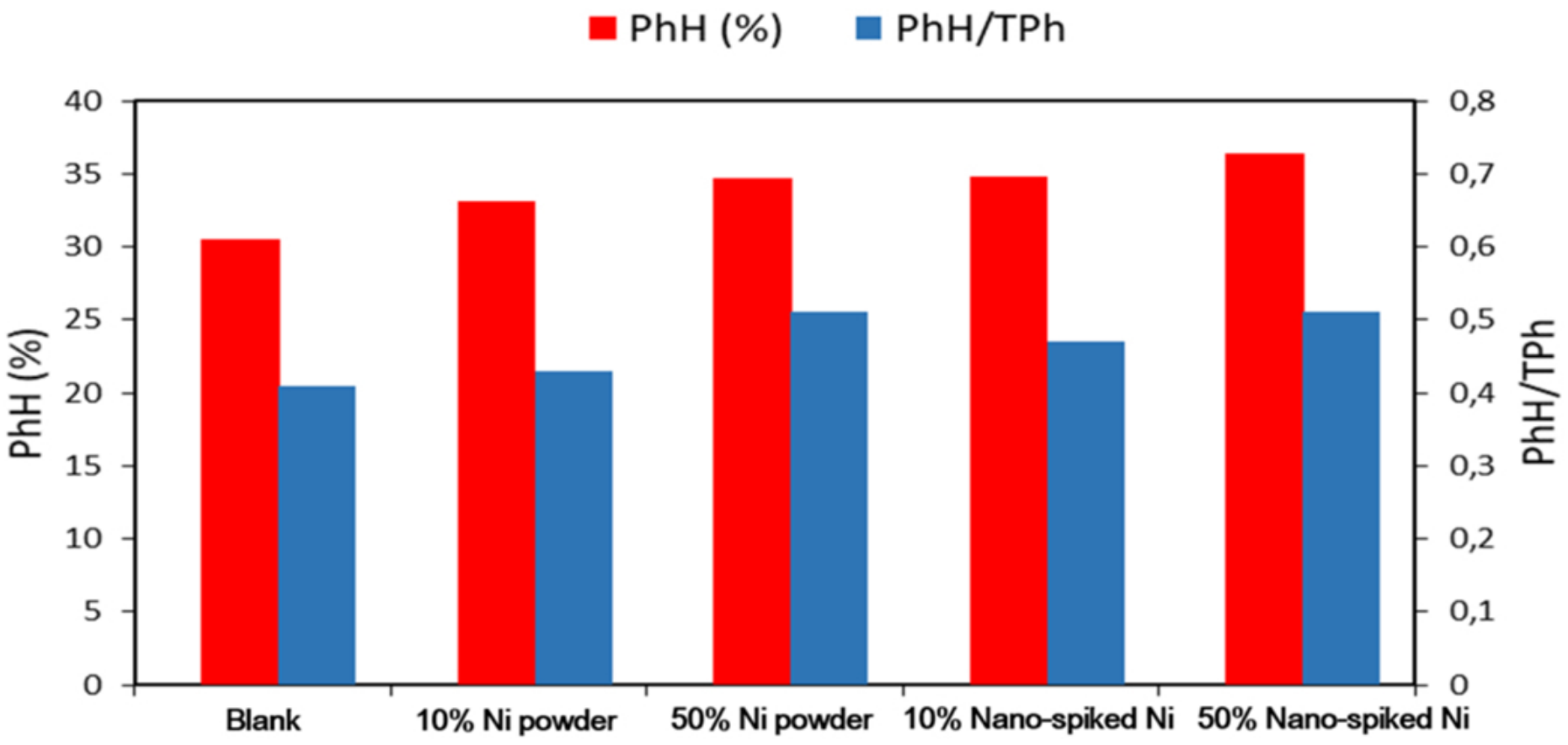
PhH (%)
PhH/TPh
40
35
30
25
20
15
10
5
0
0,8
0,7
0,6
0,5
0,4
0,3
0,2
0,1
0
PhH (%)
PhH/TPh
Blank
10% Ni powder
50% Ni powder
10% Nano-spiked Ni
50% Nano-spiked Ni

Figure 6

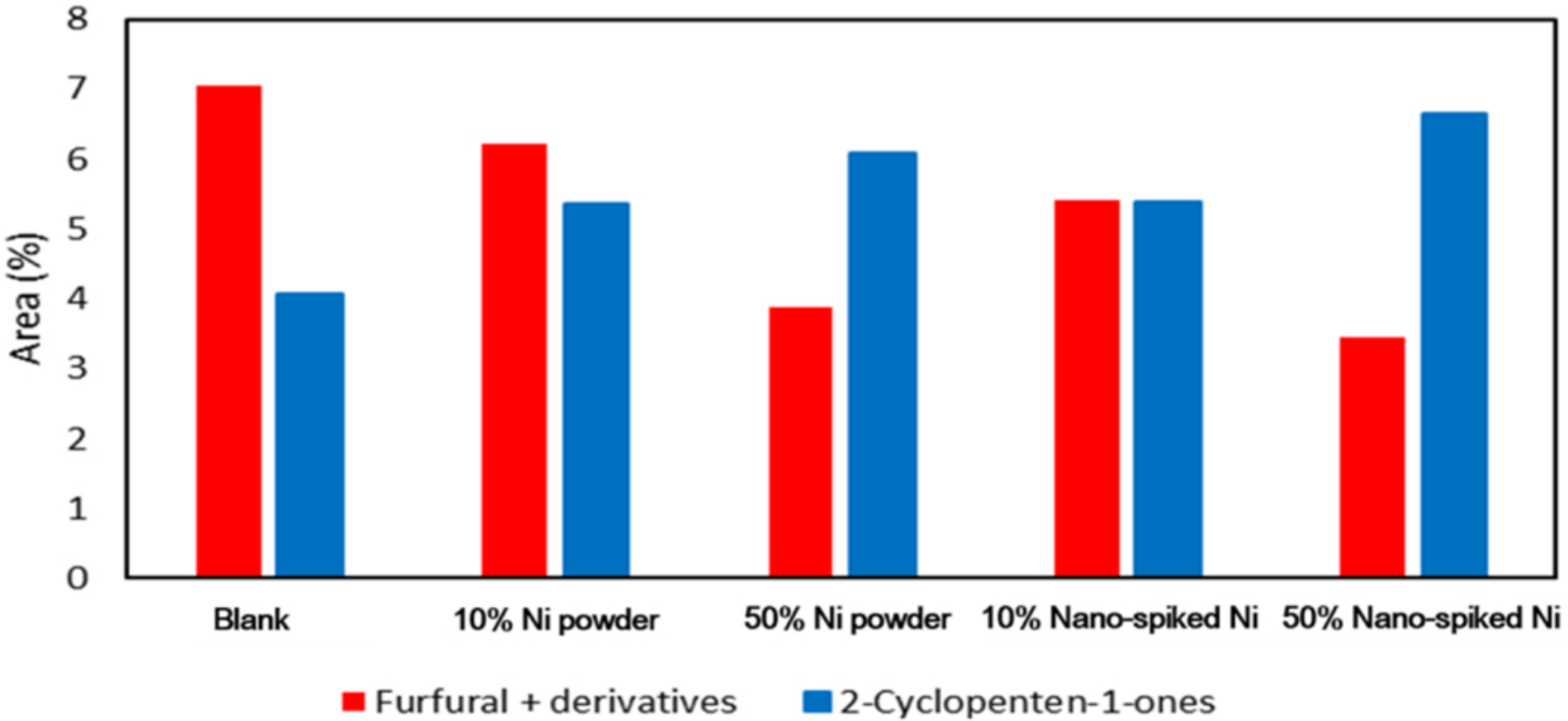
8
7
6
5
4
3
2
1
0
Area (%)
Blank
10% Ni powder
50% Ni powder
10% Nano-spiked Ni
50% Nano-spiked Ni
Furfural + derivatives
2-Cyclopenten-1-ones

Figure 7